Pattern formation induced by ion-selective surfaces: Models and simulations

Szabolcs Horvát[a)]
Department of Theoretical Physics, Babeş-Bolyai University, Str. Kogălniceanu, nr. 1/B, 400084 Cluj Kolozvár, Romania

Péter Hantz[b)]
Department of Theoretical Physics, Babeş-Bolyai University, Str. Kogălniceanu, nr. 1/B, 400084 Cluj Kolozvár, Romania and Department of Plant Taxonomy and Ecology, Etövös Loránd University, Pázmány sétány 1/C 1117 Budapest, Hungary

(Received 22 November 2004; accepted 4 May 2005; published online 27 July 2005)

Simple inorganic reactions in gels, such as $NaOH+CuCl_2$, $NaOH+AgNO_3$, and $CuCl_2+K_3[Fe(CN)_6]$, can yield to various precipitation patterns. The first compound penetrates in a hydrogel by diffusion, and reacts with the second compound homogenized in the gel. The precipitate patterns formed in these reactions have got two kinds of bordering surfaces. Recent experimental results suggested that one of these surfaces has an ion-selective (semipermeable) character: It restrains the diffusion of the reacting ion contained by the reactant that diffuses into the gel. In this paper, we built the above experimental observation into a reaction-diffusion cellular-automata model of the pattern formation. Computer simulations showed that the model is able to reproduce the basic building elements of the patterns.
 [DOI: 10.1063/1.1943409]

I. INTRODUCTION

Inorganic chemical reactions, coupled with diffusion, can lead to various types of precipitation patterns.[1] A well-known example is the Liesegang banding, where one of the reagents, the *inner electrolyte*, is homogenized in a hydrogel, while the other one, the *outer electrolyte* penetrates in the gel by diffusion. The precipitate patterns are built up behind the diffusion front of the outer electrolyte. The gel environment prohibits convection, and keeps the precipitate at the place where it formed.[2–6]

Recently, a new class of simple reactions was discovered, that, running in the above Liesegang-type setup, can yield to a great diversity of precipitation patterns.[7–10] Reactions such as $NaOH+CuCl_2$, $NaOH+AgNO_3$, and $CuCl_2+K_3[Fe(CN)_6]$ in gel columns are able to build up, among others, spirals and concentric cones of precipitate, and some kinds of irregular patterns as well. These formations are called primary patterns. The first two reactions in polyvinylalcohol hydrogel medium can also result in regular grids and sheets of precipitate with small wavelengths even in the order of 10 μm, referred to as the secondary patterns.[8]

When the reactions are running in gel sheets, it can be observed how the basic building elements of the primary patterns emerge (Fig. 1). The diffusion front of the outer electrolyte is followed by a sharp precipitation front. If some impurities or inhomogeneities are present on the gel surface or inside the gel, the precipitation may not start, or may cease at these points. As the staggered precipitation front proceeds, these centers expand into wedgelike regions free of precipitate. The reactions do not proceed on the oblique edges that separate the already formed precipitate from the wedgelike empty regions. These stationary surfaces are referred to as the *passive borders*. The precipitation front segments are referred to as the *active borders*. The shrinking active-border segments gradually vanish, and the lower limit of the precipitate will be a zigzag-shaped passive border. Reactions such as $NaOH+AgNO_3$ and $CuCl_2+K_3[Fe(CN)_6]$ running in gel layers thicker than about 1 mm stop at this point, but in some others, such as $NaOH+CuCl_2$, new precipitation fronts may start later, at the top of the wedgelike empty regions.

Recent experimental results demonstrated that the passive borders are ion-selective (semipermeable) membranes.[11] These membranes restrain the passage of those ions of the outer electrolyte that react with the inner electrolyte to form the precipitate. As a consequence, the reactions cannot proceed ahead of the passive borders. In the $NaOH+CuCl_2$ process, where precipitation can restart below the passive borders, these borders might be slightly leaking, or may become damaged. Since the active borders are permeable, ions of the outer electrolyte will cross these surfaces, and reactions will take place ahead of them.

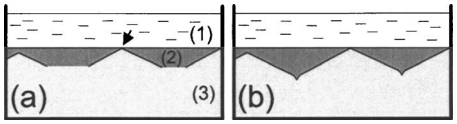

FIG. 1. The outer electrolyte (1) penetrates in the hydrogel containing the inner electrolyte (3), and precipitate (2) is forming. Passive borders are marked by black, while the active borders with white lines. (a) Snapshot of pattern formation. A point where precipitation did not start is marked by an arrow. (b) The precipitate is already formed, being delimited from below by a zigzag-shaped passive border.

[a)]Electronic mail: szhorvat@phys.ubbcluj.ro
[b)]Electronic mail: hantz@general.elte.hu

Here we mention that observation of the spontaneous formation of a cellular structure in a simple inorganic system has recently been reported. The wall of the cells consists of a semipermeable membrane.[12]

In this paper a new mathematical model of the pattern formation is presented, which is a combination of reaction-diffusion equations and a cellular automata. Our model, based on the finding that the passive borders are ion-selective membranes, is a revised version of the hypothesis presented in Ref. 9. Computer simulations showed that the new model is able to reproduce the main characteristics of the formation of primary patterns.

II. PHENOMENOLOGY

Before introducing the equations and cellular-automata rules of the model, a qualitative explanation of the most relevant experimental results will be presented.

Let us assume first that we already have a progressing active border. Conditions of its appearance will be reexamined later. Several experiments suggest that the reactions first lead to the formation of a diffusive intermediary compound (DC), and a critical concentration of this compound is required in order for the precipitation to proceed.[9,11] This concentration will be referred to as the c^* *growth threshold*. In a previous work, it was supposed that the reagents react and the DC forms only on the active border with catalytic properties.[9] In the present model, this supposition is not necessary anymore: Recent experimental results demonstrated that the passive borders of the precipitate regions are ion-selective (semipermeable) surfaces that restrain the passage of the reacting ions contained by the outer electrolyte.[11] Formation of DC is allowed in the whole region where the reagents meet, but, due to the restraining properties of the passive borders, it will arise mainly the region ahead of the active borders. Inclusion of the restraining properties of the passive borders into the model represents the main point of the present work.

Emergence of passive borders is explained as follows. If the growth threshold is not reached within a certain time τ on a portion of the precipitation front, the front portion is assumed to loose its permeability, and becomes passivized. Since the speed of the precipitation front decreases in time, a constant value of τ would entail its stoppage in a finite time. However, experimental results suggest that, having a constant outer electrolyte concentration, arbitrary long front propagation can take place.[7] This can be reproduced by assuming that $\tau=\tau(v)$ increases as the front speed v decreases.

The most important qualitative feature of the formation of primary patterns is the shrinking of active-border segments that leave behind a trapezoid-shaped precipitate area, finally evolving to a triangle of precipitate.[7,9,11] In order to explain this feature, we have to assume that the concentration of the DC does not reach the growth threshold around the end point of the active-border segment within time $\tau(v)$. Computer simulations showed that this situation is typical.

Splitting of an active border can happen when it reaches an impurity or inhomogeneity either inside or at the surface of the gel.[9] In our explanation, the impurity prohibits the encountering of the reagents, and no DC is produced. If the growth threshold is not reached within time $\tau(v)$, a portion of passive border will appear. The is referred to as the *active-passive transition*.

Here we mention that a segment of an active border that faces an obstacle, such as an air bubble or a splint of glass larger than 0.1–0.2 mm, speeds up before it touches the barrier. The speedup begins when the front is at about a 60 μm distance from the obstacle.[9] Since the DC cannot pass through the barrier, its concentration may rise between the obstacle and the front. Higher concentration of the DC is the most probable reason of the front-segment speedup.

Initiation of traveling active borders is attributed to DC concentrations above the c^{**} *nucleation threshold*, which is assumed to be higher than the growth threshold.[13] In reactions such as $NaOH+AgNO_3$ and $CuCl_2+K_3[Fe(CN)_6]$ in gel columns or gel layers thicker than about 1 mm, new active borders appear almost exclusively at the beginning of the experiment, when the outer electrolyte is layered on the gel. In the $NaOH+CuCl_2$ system, front initiation can happen in the top of the wedgelike empty regions, some time after the passive border formed and reagent concentrations are recovered by diffusion. Since the reason of this latter effect is unknown, and simple assumptions did not lead to the expected simulation results, it is not included in the present model.

III. THE MATHEMATICAL MODEL

The mathematical model is based on the most relevant experimental results presented in Refs. 7, 9, and 11. It consists of coupled reaction-diffusion equations and a cellular automata.[14–16] The latter were included in the model in order to handle the precipitate regions, which have sharp bordering surfaces. Similar cellular-automata–reaction-diffusion approach has recently been used to model chemical systems involving a long- (macroscopic) and a short- (atomic) length scale.[17]

Most elements of the model are straightforwardly derived from the experiments [existence of the DC, as well as that of active (permeable) and passive (semipermeable) stages of the precipitate], some others represent classical results of the colloid science (nucleation and growth thresholds). The assumed mechanisms of passivization are deduced from indirect observations. However, they represent the simplest assumptions that led to the patterns observed in the experiments. Equations and cellular-automata rules of the dimensionless model are the following:

$$\frac{\partial a(x,y,t)}{\partial t} = D_a(x,y)\cdot\Delta a(x,y,t) - r\cdot a(x,y,t)\cdot b(x,y,t), \qquad (1)$$

$$\frac{\partial b(x,y,t)}{\partial t} = D_b(x,y)\cdot\Delta b(x,y,t) - r\cdot a(x,y,t)\cdot b(x,y,t), \qquad (2)$$

$$\frac{\partial c(x,y,t)}{\partial t} = D_c(x,y)\cdot\Delta c(x,y,t) + r\cdot a(x,y,t)\cdot b(x,y,t) - [R], \qquad (3)$$

$$\text{(R0):}\quad [c(x,y,t) > c^{**}] \wedge [d(x,y,t) = \text{empty}] \rightarrow d(x,y,t) = \text{active},$$

$$\text{(R1):}\quad [c(x,y,t) > c^{*}] \wedge [d(x,y,t) = \text{active}] \wedge [d(x_{nn},y_{nn},t) = \text{empty}] \rightarrow [d(x_{nn},y_{nn},t+\Delta t) = \text{active}] \wedge [d(x,y,t+\Delta t) = \text{bulk precipitate}] \wedge [c(x,y,t+\Delta t) = 0],$$

$$\text{(R2):}\quad [c(x,y,t) < c^{*}] \wedge [d(x,y,t) = \text{active}] \wedge [T(x,y,t) \leqslant \tau(\upsilon)] \rightarrow T(x,y,t+\Delta t) = T(x,y,t) + \Delta t,$$

$$\text{(R3):}\quad [c(x,y,t) < c^{*}] \wedge [d(x,y,t) = \text{active}] \wedge [T(x,y,t) > \tau(\upsilon)] \rightarrow d(x,y,t+\Delta t) = \text{passive},$$

$$\text{(R4):}\quad [d(x,y,t) = \text{active}] \wedge [d(x_{nn},y_{nn},t) = \text{nonempty}\ \forall\ (x_{nn},y_{nn})] \rightarrow d(x,y,t+\Delta t) = \text{bulk precipitate},$$

$$D_a(x,y) = \begin{cases} 0, & \text{if } d(x,y) = \text{passive or obstacle} \\ D_a, & \text{otherwise,} \end{cases}$$

$$D_{b,c}(x,y) = \begin{cases} 0, & \text{if } d(x,y) = \text{nonempty} \\ D_{b,c}, & \text{otherwise.} \end{cases}$$

Coordinates of the reaction field, which correspond to a gel sheet, are denoted by x and y, while t denotes time and Δt the time step. The terms $a(x,y,t)$ and $b(x,y,t)$ represent the reacting ions of the outer and inner electrolytes, $c(x,y,t)$ the diffusive intermediary compound DC, c^{**} the nucleation threshold, and c^{*} the growth threshold. $[R]$ symbolizes the coupling with the cellular-automata rules.

The term $d(x,y,t)$, denoting the precipitate, is not related to concentrations. It can take just a few (arbitrary) values, denoting the bulk precipitate, the active borders, the passive borders, as well as the "empty" regions free of precipitate. The obstacles are inert cells, where none of the compounds can penetrate by diffusion.

$T(x,y,t)$ represents the age, while $\tau(\upsilon)$ the maximal lifetime of the cells, where υ denotes the speed of the precipitation front. In general, the maximal lifetime is assumed to depend on the front speed υ. Nearest neighbors of the cell at the lattice point (x,y) are denoted by (x_{nn},y_{nn}). The symbol "$\wedge$" represents the logical "AND".

Initially, the reaction field contains only the compound b having a uniform concentration b_0, as well as some inert and semipermeable obstacles. Reagent a has the concentration a_0 along the $x=0$ edge, and zero-flux boundary conditions on the other edges of the reaction field. All the other compounds have zero-flux boundary conditions on the entire edge of the reaction field.

The Laplace operator in the diffusion term is denoted by Δ. Diffusion coefficients of the reagents in the regions free of precipitate are D_a and D_b, that of the DC is D_c. In our model, the diffusion coefficient of the outer electrolyte is zero on the passive borders, that is, it cannot cross these surfaces. The inner electrolyte is unable to diffuse in the precipitate. However, alterations of D_b on the passive borders as well as in the bulk precipitate do not change the character of the simulation results. The precipitate cannot diffuse at all. The reaction, having rate r, is supposed to be proportional to the reagent concentrations.

The meaning of the cellular-automata rules are the following:

Appearance of new precipitation fronts is encoded by rule 0. If in a point of the reaction field there is no precipitate or obstacle (empty point), and concentration of c exceeds the nucleation threshold c^{**}, new front segments (active cells) appear.

Rule 1 describes the progress of an active border. If the concentration of the DC exceeds the growth threshold c^{*} at a cell of the active border, all the nearest neighbors of the cell which are empty become active. On a square lattice these are the first Neumann-type neighbors. The DC is assumed to be consumed during the activation process, and therefore it is eliminated from a cell that activated its surrounding.

The model assumes that only the surface of the precipitate can act as a region where precipitation can happen. Therefore, the cell that has activated its surrounding has to become passive. This consequence is also included in rule 1.

Rules 2 and 3 implement the assumption that the concentration of the DC has to reach the growth threshold c^{*} within time $\tau(\upsilon)$ measured from the emergence of the active cell, otherwise the element will be passivized. Aging of the cell is described by rule 2, and passivization at the end of its lifetime is governed by rule 3. Investigated forms of the function $\tau(\upsilon)$ are discussed in Sec. IV.

Rule 4 describes the second way of passivization, which is an extension of the passivization algorithm of rule 1. Cells of the active border are passivized in any configuration, when they become surrounded by either active or passive cells. Note that an active cell surrounded by precipitated cells and portions of the obstacle also gets passivized.

In the computational implementation of the model, the differential equations are applied first, the cellular-automata rules afterwards. The rules act in the order R0-R1-R2-R3-R4.

Progression of the active borders goes on in the following way: The reaction produces the DC, while reagents a and b are depleted in the surrounding. Since the outer electrolyte cannot cross the passive borders, the reaction is taking place mainly ahead of the active borders. Due to the reaction, concentration of DC will rise at the active border, while age T of the cells of at front is also increasing. Let us assume that the growth threshold c^{*} is reached before the age of the cells exceeds the lifetime $\tau(\upsilon)$. Usually this happens at the same

time in a larger front segment. At this moment, the first neighbors of the active cells (which in this configuration are the next row of cells) become active, while the "mother cells" get passivized. At the same time DC gets depleted in the passivized cells, but while its diffusion rate for the passivized cells is zero, the magnitude of DC in these cells has no influence on the simulation results.

Splitting of an active border in segments may happen when it overtakes an obstacle. In order for the splitting to occur, the concentration of DC around the end points of the active-border segments has to be lower than the constant value in the middle of them. In this case, the active cells around the end points will not be able to activate their surrounding when the central segment of the front does. However, these cells remain permeable for the outer electrolyte, but at appropriate parameter values the growth threshold c^* will not be reached along them in their lifetime $\tau(v)$. As a consequence, they will be passivized when their age T reaches $\tau(v)$.

In order for the shrinking of active-border segments to occur, the concentration of DC around their end points has to be permanently lower than the constant value in the middle. Computer simulations showed that this situation is typical for a wide range of parameters. Due to the mechanism presented above, the cells around their end points are getting passivized, the active-border segments are shortened, and finally disappear, leaving behind precipitate triangles.

In order to increase numerical precision, decreasing the mesh size of the space discretization may appear desirable. However, if physical parameters have to be kept constant, rules 1 and 4 need to be changed. Several rows of active cells have to emerge at the same time, and not only the border cells can be active. Such extensions of the model have not been investigated. Decreasing of the time step does not cause similar problems.

IV. SIMULATION RESULTS

Computer simulations were performed on a rectangular grid using the finite-volume method. The boundary conditions are described in Sec. III. The size of the time step was 0.05 while that of the mesh size was 1.0. Since the detailed chemical mechanism of the reactions is unknown at the moment, the parameters are not experimentally measured values.

Two versions of the model were investigated, namely, when $\tau(v)$ is constant or has a simple dependence on the front speed v. In both cases, the active border arise at the $x=0$ edge just after the simulations were started. In order to initiate front splitting, two obstacles were placed at equal distances from the $x=0$ edge. When the precipitation front overtakes the obstacles, an active-passive transition can occur: The active border splits and begins to shrink, leaving behind a trapezoid-shaped precipitate region that finally evolves into a triangle.

Although the version when $\tau(v)$ is constant is able to reproduce formation of precipitate triangles (Fig. 2), it has a major disadvantage. Except some transients, position x of the precipitation front increases with time as $x \propto \sqrt{t}$, and the

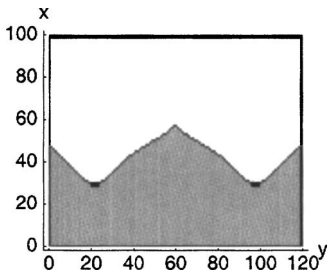

FIG. 2. Precipitate triangle formed when $\tau(v)$ is constant. The simulation was performed on a rectangular grid of 120×100 units. Dark gray represents the bulk precipitate, and light gray the regions free of precipitate. Passive borders and obstacles are drawn in black, while the active borders in white. The parameters are the following: $D_a=3.0$, $D_b=1.0$, $D_c=0.3$, $r=0.1$, $c^{**}=11.0$, $c^*=10.0$, $\tau=8.0$, $a_0=40.0$, and $b_0=10.0$. The obstacles are rectangles of 4×2 units, placed at $x=30$, $y=22$, and $y=98$, respectively. Note that a small cusp, referred to as the "Meinhardt peak" is formed at the top of the precipitate triangle. The mechanism of cusp formation has not been investigated in detail.

speed v of the front is proportional to $1/\sqrt{t}$. The age T at which the active cells are passivized is inversely proportional to v, consequently $T \propto x$. Therefore at some distance x the age T reaches τ, a passive border forms and the front stops. Thus, when τ is constant, the front is unable to travel to an arbitrary distance, while experimental findings indicate the contrary. Moreover, the parameter range where formation of triangle-like patterns occurs is thin. This problem can be avoided in the simplest way by setting the lifetime $\tau(v)$ of an active cell to $T_{\text{previous}}+\tau_0$, where T_{previous} is the age of the mother cell that activated it, and τ_0 is a positive constant. The addition of τ_0 is necessary because the newly activated cells need more time to reach c^* than their mother cells did. This kind of $\tau(v)$ is capable of producing triangles of an arbitrary size, in a wide range of parameters (Fig. 3). Note that the bending of reaction fronts when facing a small obstacle has also been observed. The results do not change significantly if diffusion of the inner electrolyte is allowed in the precipitate with a reduced, but nonzero rate.

Finally, we mention that similar patterns can be obtained using an alternative model in which the outer and inner electrolytes react to form a precipitate. In this model, the precipitate can have different concentrations, and at appropriate parameter values, it will have an increased value around the end points of the active border. By assuming that above a concentration threshold the precipitate is semipermeable, formation of the triangular patterns has also been achieved.

V. DISCUSSION AND OPEN QUESTIONS

Computer implementations of the mathematical models presented above are able to reproduce the main features of the formation of primary patterns: front initiation at the beginning of the experiments, front splitting, as well as the development of trapezoid-shaped regions that finally evolve to triangles of precipitate. Thus, it is shown that the existence of the passive (semipermeable) borders can naturally lead to a special distribution of the DC, its concentration being smaller around the end points of the active borders, and, as a consequence, to the formation of the triangular precipitate patterns observed in the experiments.

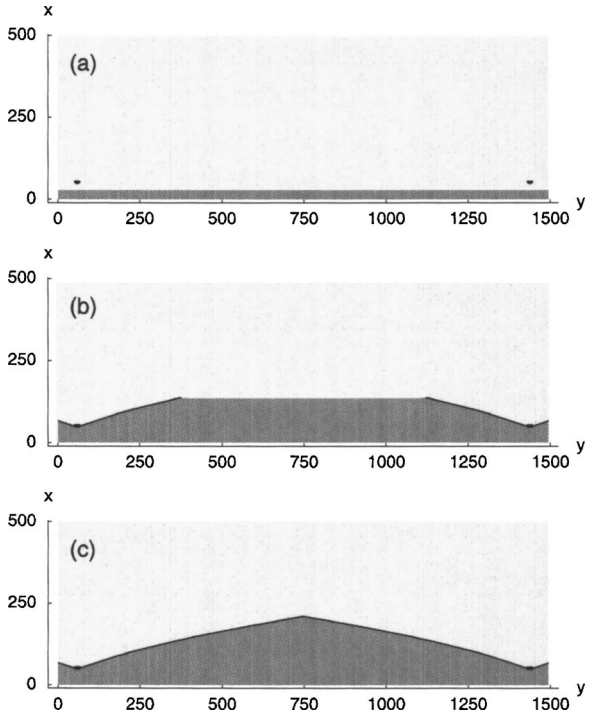

FIG. 3. Precipitate triangle formed when $\tau(v)=T_{\text{previous}}+\tau_0$. The simulation was performed on a rectangular grid of 1500×500 units. The meaning of the colors is the same as in Fig. 2. The obstacles are semicircles with radii of 10 units placed at $x=60$, $y=60$, and $y=1440$, respectively. The parameters are the following: $D_a=3.0$, $D_b=1.0$, $D_c=0.8$, $r=0.1$, $c^{**}=9.0$, $c^{*}=7.0$, $\tau_0=2.0$, $a_0=40.0$, and $b_0=10.0$. The thickness of the active and passive borders has been enhanced on this figure. (a) The traveling precipitation front shortly after it appeared. The time elapsed from the beginning of the simulation is $t=90$. (b) A trapezoid-shaped precipitate region is growing in the central area, having a shrinking active border. Note the short transient (the passive border is slightly bent) in the vicinity of the obstacles that caused the active-passive transition. The time elapsed is $t=1480$. (c) The reactions are over; the precipitate triangle has been completed.

A previous model was also able to reproduce the formation of precipitate triangles, but only under very peculiar circumstances. It was assumed that both reagents are initially present in the reaction field.[9] Moreover, the reaction could take place only on the active border, having catalytic properties. The new model has more accurate assumptions: The outer electrolyte is gradually carried by diffusion into the reaction field, the reagents immediately react as they meet, and the diffusive intermediary compound is formed. The improved model does not require the existence of catalytic precipitate surfaces, only those with semipermeable properties, already found in the experiments reported in Ref. 11. Note that inorganic semipermeable membranes have been observed in various precipitation reactions.[12,18] The new model includes nucleation, and it is able to describe precipitation front propagation with variable speed, which were missing from the previous explanation.

In spite of the differences, the rationale of both pattern-forming mechanisms is the same: The concentration of a diffusive intermediary compound, necessary for the further production of the precipitate, is smaller around the margin of an active precipitate area. It is important to mention that this decrease has essentially different grounds in the previous and the new model.

However, the experiments performed up to this time could not explore the whole reaction mechanism. Beside others, the nature of passive-border formation is unclear. Regarding to the hypothesis of "aging," its microscopic explanation is unknown, as well as the dependence of the lifetime $\tau(v)$ on the front speed. The molecular mechanism of the ion selectivity of the passive borders has not been revealed. The passive borders may only restrain the diffusion of the outer electrolyte's reacting ion, or may prohibit the crossing of some other species of ions as well.

As mentioned earlier, slightly different versions of the model led to the same ability of reproducing the front initiation and pattern formation. This shows that the model has a remarkable robustness.

ACKNOWLEDGMENTS

We are indebted to P.-G. de Gennes and Z. Rácz for useful discussions. This work was supported by grant NKFP 3A/0036/2002, the Domus Hungarica Foundation of the Hungarian Academy of Sciences, the Agora Foundation, Sapientia-KPI Foundation, and the Apáczai Foundation of the Hungarian Ministry of Education.

[1] S. Müller and J. Ross, J. Phys. Chem. A **107**, 7997 (2003).
[2] S. Kai, S. Müller, and J. Ross, J. Chem. Phys. **76**, 1392 (1982).
[3] T. Antal, M. Droz, J. Magnin, Z. Rácz, and M. Zrínyi, J. Chem. Phys. **109**, 9479 (1998).
[4] A. Büki, E. Kárpáti-Smidróczki, and M. Zrínyi, J. Chem. Phys. **103**, 10387 (1995).
[5] T. Antal, M. Droz, J. Magnin, and Z. Rácz, Phys. Rev. Lett. **83**, 2880 (1999).
[6] M. Fialkowski, A. Bitner, and B. Grzybowski, Phys. Rev. Lett. **94**, 018303 (2005).
[7] P. Hantz, J. Phys. Chem. B **104**, 4266 (2000).
[8] P. Hantz, Phys. Chem. Chem. Phys. **4**, 1262 (2002).
[9] P. Hantz, J. Chem. Phys. **117**, 6646 (2002).
[10] B. de Lacy Costello, P. Hantz, and N. Ratcliffe, J. Chem. Phys. **120**, 2413 (2004).
[11] P. Hantz, J. Partridge, G. Láng, S. Horvát, and M. Ujvári, J. Phys. Chem. B **108**, 18135 (2004).
[12] J. Maselko and P. Strizhak, J. Phys. Chem. B **108**, 4937 (2004).
[13] R. Hunter, *Introduction to Modern Colloid Science* (Oxford University Press, Oxford, 1993).
[14] J. H. Ferzinger and M. Peric, *Computational Methods for Fluid Dynamics* (Springer, Berlin, 1996).
[15] J. R. Weimar and J.-P. Boon, Phys. Rev. E **49**, 1749 (1994).
[16] B. Chopard and M. Droz, *Cellular Automata Modeling of Physical Systems* (Cambridge University Press, Cambridge, 1998).
[17] L. Pismen, M. Monine, and G. Tschernikov, Physica D **119**, 82 (2004).
[18] J. H. E. Cartwright, J. M. García-Ruiz, M. L. Novella, and F. Otálora, J. Colloid Interface Sci. **256**, 351 (2002).